doi:10.1093/brain/awz053 BRAIN 2019: 142; 1334–1348 | 1334

BRAIN
A JOURNAL OF NEUROLOGY

Neurological toxicities associated with chimeric antigen receptor T-cell therapy

Daniel B. Rubin,[1,2] Husain H. Danish,[1,2] Ali Basil Ali,[1] Karen Li,[1] Sarah LaRose,[1] Andrew D. Monk,[1] David J. Cote,[3] Lauren Spendley,[4] Angela H. Kim,[1] Matthew S. Robertson,[5] Matthew Torre,[6] Timothy R. Smith,[7] Saef Izzy,[1] Caron A. Jacobson,[4] Jong Woo Lee[1] and Henrikas Vaitkevicius[1]

Chimeric antigen receptor T cell therapy has become an important tool in the treatment of relapsed and refractory malignancy; however, it is associated with significant neurological toxicity. We characterized the neurological toxicity associated with chimeric antigen receptor T-cell therapy in a consecutive series of 100 patients up to 2 months post transfusion, 28 of whom were obtained from chart review and the others by prospective observation. The underlying neoplasms were lymphoma (74%), myeloma (14%), leukaemia (10%), and sarcoma (2%). The median age of the cohort was 64.5 years old and 39% of patients were female. The most commonly occurring neurological symptoms were encephalopathy (57%), headache (42%), tremor (38%), aphasia (35%) and focal weakness (11%). Focal neurological deficits are frequently observed after chimeric antigen receptor T-cell therapy and are associated with regional EEG abnormalities, FDG-PET hypometabolism, and elevated velocities on transcranial Doppler ultrasound. In contrast, structural imaging was typically normal. As this form of treatment is more widely adopted, recognition of the frequently encountered symptoms will be of increasing importance for the neurologists and oncologists caring for this growing patient population.

1 Department of Neurology, Brigham and Women's Hospital, Harvard Medical School, Boston, MA, USA
2 Department of Neurology, Massachusetts General Hospital, Harvard Medical School, Boston, MA, USA
3 Department of Neurosurgery; Channing Division of Network Medicine, Brigham and Women's Hospital, Harvard Medical School, Boston, MA, USA
4 Department of Medical Oncology, Dana-Farber Cancer Institute, Harvard Medical School, Boston, MA, USA
5 Division of Nuclear Medicine, Department of Radiology, Brigham and Women's Hospital, Harvard Medical School, Boston, MA, USA
6 Department of Pathology, Brigham and Women's Hospital, Harvard Medical School, Boston, MA, USA
7 Department of Neurosurgery, Brigham and Women's Hospital, Harvard Medical School, Boston, MA, USA

Correspondence to: Henrikas Vaitkevicius
75 Francis Street, Boston, MA, USA 02115
E-mail: hvait@bwh.harvard.edu

Keywords: neurotoxicity; CAR T cells; immunotherapy

Abbreviations: ACA = anterior cerebral artery; CAR = chimeric antigen receptor; CRS = cytokine release syndrome; CTCAE = Common Terminology Criteria for Adverse Events; FDG = ^{18}F-fluorodeoxyglucose; MCA = middle cerebral artery; PCA = posterior cerebral artery; RDA = rhythmic delta activity

Received October 23, 2018. Revised December 21, 2018. Accepted January 18, 2019. Advance Access publication March 19, 2019

Introduction

Chimeric antigen receptor (CAR) T cells have emerged in recent years as a powerful treatment for relapsed and refractory haematological malignancies (Brudno and Kochenderfer, 2018). Impressive therapeutic response rates, however, are accompanied by significant and often treatment-limiting toxicity (Neelapu *et al.*, 2017; Gutierrez *et al.*, 2018). Toxicity predominately occurs as two related but distinct syndromes: cytokine release syndrome (CRS) and neurotoxicity.

CRS is a multi-system clinical syndrome characterized by fever, hypotension, hypoxia, and in more severe cases multisystem organ dysfunction (Gutierrez *et al.*, 2018). CRS is caused by the widespread release of pro-inflammatory cytokines by the activated CAR T cells (Brudno and Kochenderfer, 2018). CRS is extremely common; in some trials, 100% of patients experienced at least some symptoms of CRS (Grupp *et al.*, 2013; Maude *et al.*, 2014). Treatment with tocilizumab, which blocks the IL-6 signal receptor pathway, can effectively mitigate the symptoms of CRS without impairing the antitumour efficacy of the CAR T cells (Neelapu *et al.*, 2017).

In contrast, the neurotoxicity associated with CAR T-cell therapy remains idiosyncratic and poorly characterized. In the literature, patients are described as variably suffering from encephalopathy, confusional state, delirium, or mental-status changes, generally without further characterization (Neelapu *et al.*, 2017; Schuster *et al.*, 2017). Other neurotoxicities, including aphasia, tremor, ataxia, seizure, and cerebral oedema, have all also been reported with varying frequency and in incomplete detail. Despite the use of the National Cancer Institute Common Terminology Criteria for Adverse Events (CTCAE v4.03) to grade symptoms, the unpredictability of neurological symptoms encountered in this population remains a source of great anxiety for patients and practitioners alike. Furthermore, the underlying pathophysiology of CAR T-associated neurotoxicity remains uncertain, and treatments that are efficacious against CRS are often of limited benefit to patients with neurotoxicity (Maude *et al.*, 2014; Kochenderfer *et al.*, 2015; Turtle *et al.*, 2016*a*; Brudno and Kochenderfer, 2018). In some cases, anti-CRS treatments, in particular tocilizumab, may even worsen neurotoxicity (Lee *et al.*, 2014; Neelapu *et al.*, 2018).

The goal of this study is to characterize the clinical features and diagnostic studies associated with neurological symptoms after CAR T-cell therapy, both to aid practitioners as well as advance our understanding of the pathophysiological mechanisms underlying these symptoms. We catalogued the neurological symptoms experienced by the first 100 consecutive patients undergoing CAR T-cell therapy at Brigham and Women's Hospital/Dana Farber Cancer Institute (BWH/DFCI) from 2015 to 2018.

Materials and methods

Between April 2015 and September 2018, all patients admitted to BWH/DFCI for CAR T-cell therapy were prospectively identified and monitored for CRS and neurotoxicity in accordance with established clinical trial/treatment protocols. Patients admitted for clinical trials as well as those admitted (following FDA approval) for administration of commercially produced CAR T-cell products were included in this series. Patients were screened prior to treatment for significant medical comorbidities; treatment inclusion/exclusion criteria are provided in the Supplementary material. For patients treated from April 2015 through February 2017 (28 patients), charts were retrospectively reviewed. All patients admitted for treatment from March 2017 through September 2018 (72 patients) were followed prospectively from the time of admission for CAR T-cell infusion through to discharge by a board-certified neurologist, and charts were then reviewed from discharge up to 2 months post treatment. No patients admitted for CAR T-cell therapy were excluded from this study. All neurological symptoms documented in daily progress notes, clinic notes, consult notes, and discharge summaries were catalogued, and all neuroimaging and other neurodiagnostic studies performed during the 2-month time interval were reviewed. CRS and neurotoxicity grades were assigned either by the individual study Principal Investigator or the inpatient attending oncologist (Supplementary Tables 1 and 2). Neurological symptoms were documented either by the attending oncologist, hospitalist, or consulting neurologist. This study was approved by the local institutional review board (IRB #2018P000227) and in compliance with STROBE Statement (von Elm *et al.*, 2007). Imaging methods and laboratory monitoring methods are provided in the Supplemental material.

Statistical analysis

Mean values of transcranial Doppler ultrasound velocities between groups were compared using an unpaired two-sample two-tailed Student's *t*-test. Median values of laboratory data between groups were compared using a two-tailed Mann-Whitney U-test. For laboratory tests with repeated values over multiple days [specifically C-reactive protein (CRP) level], a linear mixed-effects model was used to compare groups, allowing a random intercept per subject. This model takes in to account the within-subject correlation of CRP levels over time. Two linear mixed-effects models were fit to the time-series data, one with a toxicity main effect term and toxicity-by-day interaction terms, and one without these terms. The two models were then compared with a likelihood ratio test. To assess for correlations between laboratory values and toxicity grades, linear regression was performed, using an F-test to evaluate for statistical significance. Data analysis was performed using R version 3.4.1 (R Core Team, 2017). P-values < 0.05 were considered statistically significant.

Data availability

Data are available for review upon request.

Results

Patient population

A total of 100 consecutive patients receiving CAR T-cell treatments were identified. Three patients underwent a

Table 1 Patient and clinical characteristics

	n		*n*
Patient characteristics			
Total number of patients	100	**Diagnoses**	
Male	61	Lymphoma	74
Female	39	Myeloma	14
		Leukaemia	10
		Sarcoma	2
Clinical characteristics			
Symptoms		**CRS (max)**	
Encephalopathy	57	Grade 1	30
Headache	42	Grade 2	34
Tremor	38	Grade 3	9
Aphasia	35	Grade 4	2
Somnolence	21	Grade 5	2
Agitated delirium	15	**Neurotoxicity (max)**	
Focal weakness	11	Grade 1	15
Rigors	11	Grade 2	13
Asterixis	8	Grade 3	17
Scotoma	5	Grade 4	2
Abulia	4	Grade 5	1
Allodynia	3	**Diagnostic studies**	
Apraxia	3	CT head	48
Scintillation	3	EEG	36
Stroke	2	TCD	31
Intracranial haemorrhage	2	MRI brain	29
Autonomic instability	2	CTA/MRA	26
Seizure	1	Lumbar puncture	14
Death	5[a]	PET brain	6

[a]Two deaths occurred due to disease progression ⩾6 weeks after CAR T cell infusion and were unlikely related to CAR T cell-associated toxicity. CTA = CT angiography; MRA = magnetic resonance angiography; TCD = transcranial Doppler.

second infusion of CAR T cells. All patients in this series were adults; ages ranged from 21 to 78 years old and the median age was 64.5 years old. Thirty-nine patients were female. The most common treatment diagnosis was lymphoma (74%), followed by multiple myeloma (14%), leukaemia (10%), and sarcoma (2%) (Table 1).

Cytokine release syndrome and neurotoxicity

CRS was observed in 77% of patients; the median day of onset was treatment Day 1 (range 0–7), and the median day of peak severity was treatment Day 4 (Fig. 1A). The median CTCAE grade of maximum CRS severity was 2, and median duration of CRS symptoms was 6 days. At least one symptom of neurotoxicity was observed in 77 patients. Mild neurological symptoms were observed but not CTCAE gradable. In cases in which neurotoxicity was specifically graded (48 patients), the median date of onset was treatment Day 6 (range 1–34 days), the median day of peak toxicity was treatment Day 8, and the median duration of neurotoxicity symptoms was 8.5 days (Fig. 1A). The median severity of CTCAE neurotoxicity was grade 2.

All 48 patients with neurotoxicity had CRS. Earlier onset of CRS was associated with greater likelihood of developing neurotoxicity and with higher neurotoxicity grade. The median date of CRS onset in patients who developed neurotoxicity was Day 1 versus Day 4 in patients who did not develop neurotoxicity ($U = 407.5$, $P = 0.0015$, two-tailed Mann-Whitney U-test) (Fig. 1B), and the median date of CRS onset in patients with neurotoxicity ⩾ grade 3 was Day 1 versus Day 2 in patients who had no neurotoxicity or neurotoxicity ⩽ grade 2 ($U = 406.5$, $P = 0.049$, two-tailed Mann-Whitney U-test) (Fig. 1C). Similarly, the serum level of C-reactive protein (CRP), which is frequently used as a biomarker of CRS in CAR T-cell therapy (Lee *et al.*, 2014) peaked significantly earlier (median Day 3 versus Day 5, $U = 855.5$, $P = 0.0060$, two-tailed Mann-Whitney U-test) in patients who developed neurotoxicity compared to those that did not (Fig. 1D). Additionally, both the baseline and peak CRP levels were significantly higher in patients who developed neurotoxicity compared to those that did not (median baseline CRP 36.7 mg/l versus 12.15 mg/l, $U = 817$, $P = 0.0027$, two-tailed Mann-Whitney U-test; median peak CRP 163.9 mg/l versus CRP 92.5 mg/l, $U = 766$, $P = 0.0008$, two-tailed Mann-Whitney U-test). Comparing two linear

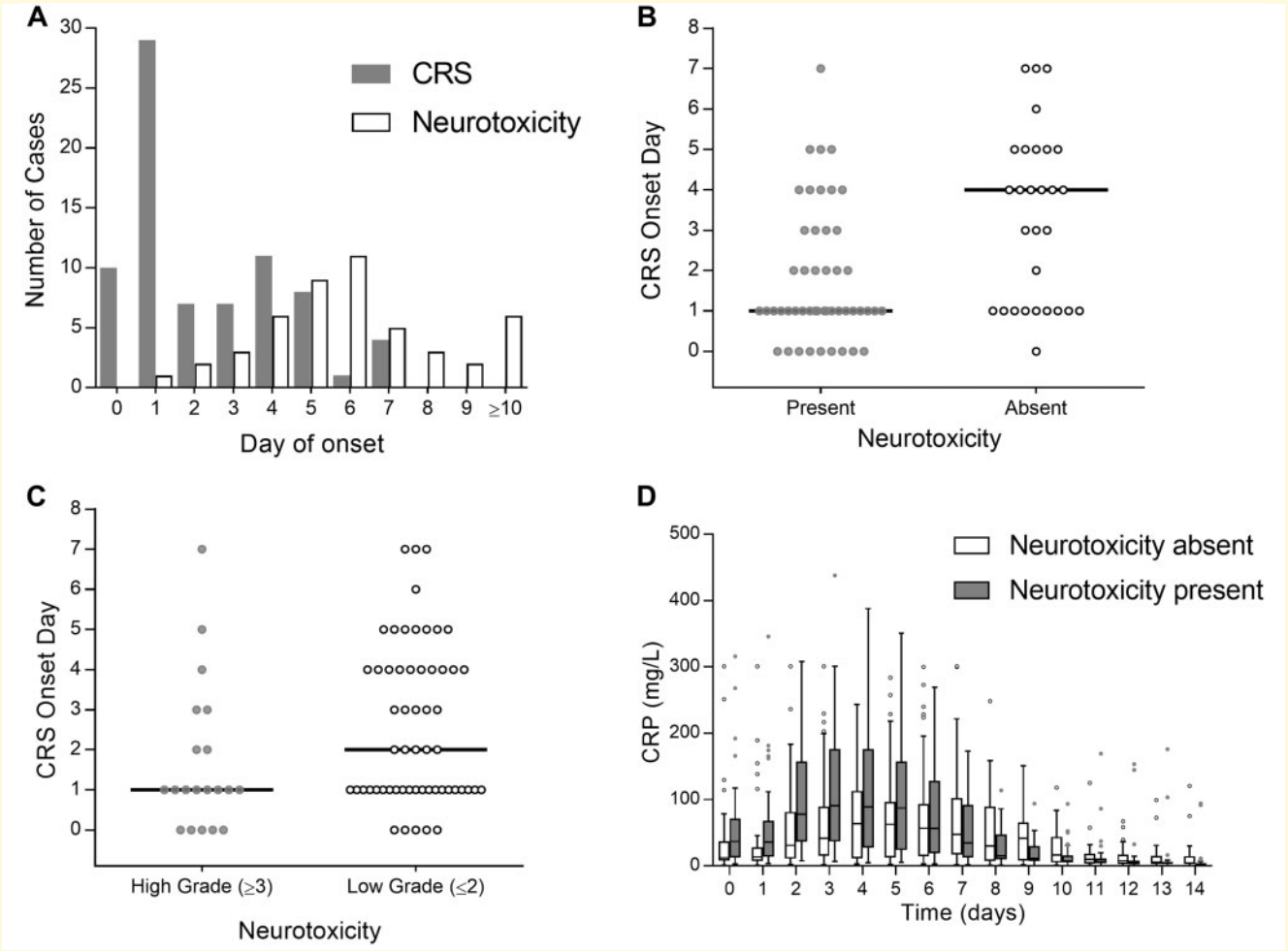

Figure 1 The association between onset of CRS and neurotoxicity. (**A**) Histogram showing day of onset (relative to CAR T-cell infusion on Day 0) for CRS (grey bars) and neurotoxicity (open bars). (**B**) Scatter dot plot of CRS onset day for patients that did (filled circles) and did not (open circles) develop neurotoxicity. Horizontal line indicates median of each group. (**C**) Scatter dot plot of CRS onset day for patients that developed severe (⩾grade 3) neurotoxicity (filled circles) versus mild/no (⩽grade 2) neurotoxicity (open circles). (**D**) Serum level of CRP in patients that did (shaded boxes/circles) and did not (open boxes/circles) develop neurotoxicity during the first two weeks post-transfusion. Box (whiskers) shows median ± 1.0 interquartile (1.5 interquartile) range. Patients who developed neurotoxicity had earlier onset of CRS, had higher baseline and peak serum levels of CRP, and had serum levels of CRP that peaked earlier than in patients who did not develop neurotoxicity.

mixed-effects models with a likelihood ratio test, we found that there was a significant interaction between daily CRP value and the presence/absence of neurotoxicity ($\chi^2 = 82.629_{15}$, $P = 2.301 \times 10^{-11}$, likelihood ratio test). We did not observe a significant correlation between baseline or peak serum CRP level and neurotoxicity grade [peak CRP versus neurotoxicity grade: $r^2 = 0.07477$, $F(1,4) = 0.3232$, $P = 0.6001$, F-test; baseline CRP versus neurotoxicity grade: $r^2 = 0.1266$, $F(1,4) = 0.5799$, $P = 0.4888$, F-test]. The three patients that died in the setting of severe CAR T-cell-associated toxicity had onset of CRS on Days 0, 1, and 2 and peak CRP values of 259.4 mg/dl, 229.7 mg/dl, and 133.8 mg/dl, respectively.

Serum levels of IL-6, a pro-inflammatory cytokine targeted in the treatment of CRS (Lee *et al.*, 2014; Neelapu *et al.*, 2018; Norelli *et al.*, 2018), were monitored in a recently treated subset of 11 patients. Of the six of these patients who developed neurotoxicity, peak IL-6 levels were greater than assay (>400 pg/ml) in four cases and >20 pg/ml in all cases (upper limit of normal is 1.8 pg/ml). Of the five of these patients who did not develop neurotoxicity, only one had a peak IL-6 level greater than assay, and the peak level was <20 pg/ml in three cases. No significant difference was observed in the peak white blood cell count or absolute neutrophil count between patients who did or did not experience CRS (median peak white blood cell count 7.38 K/ml versus 5.80 K/ml, U = 737, $P = 0.6273$, two-tailed Mann-Whitney U-test; median peak absolute neutrophil count 6298/ml versus 4507/ml, U = 624, $P = 0.1582$, two-tailed Mann-Whitney U-test) or

neurotoxicity (median peak white blood cell count 7.02 K/ml versus 7.81 K/ml, U = 1057, $P = 0.7249$, two-tailed Mann-Whitney U-test; median peak absolute neutrophil count 6298/ml versus 5470/ml, U = 990, $P = 0.4932$, two-tailed Mann-Whitney U-test).

Generalized neurological symptoms

Encephalopathy: confusion/agitated delirium/somnolence/abulia

The most common neurological symptom was generalized encephalopathy, observed in 57 cases. Encephalopathy was most often characterized as a state of waxing and waning inattentiveness with or without accompanying confusion, disorientation, impulsivity, and emotional lability. A depressed level of arousal, ranging from mild somnolence to significant lethargy with difficulty arousing, was noted in 21 cases. Agitated delirium, accompanied by increased impulsivity and aggression, was observed in 15 cases. Four patients were specifically described as abulic.

Although the encephalopathy of CAR T-cell neurotoxicity is often described as occurring as one of a variety of different syndromes (e.g. 'confusional state', 'delirium', 'cognitive impairment', 'memory impairment', 'somnolence', and 'mental-status changes' (Neelapu *et al.*, 2017; Schuster *et al.*, 2017), in our cohort, encephalopathy was observed as a single entity with a wide spectrum of severity. Patients with milder symptoms often had only slight memory impairment, disorientation, attentional deficits, or difficulty following multi-step commands. More severe syndromes manifested as periods of frank agitated delirium requiring the use neuroleptics or obtundation requiring intubation for airway protection. When present, these severe symptoms tended to evolve from more mild syndromes over the course of days. In some instances, however, severe encephalopathy presented abruptly. As patients recovered from severe encephalopathy, they would recapitulate symptoms of their milder syndrome before recovering completely. Language dysfunction was frequently co-encountered and is described below. During early periods of CAR T cell-associated encephalopathy, patients were often found to have symptoms of frontal lobe dysfunction including positive frontal release signs on neurological exam, such as palmomental, snout, and grasp reflexes.

Headache

Headache was reported in 42 cases. Headaches were usually mild in severity; in only eight cases was headache described as 'severe', 'excruciating', or greater than 7/10 in severity. Headache quality was most often 'tension-like' or 'pressure-like', and was located either diffusely or over a specific area, most commonly the occiput. Migrainous features, such as throbbing quality, photo/phonophobia, or transient visual obscurations, were described in five cases (including one case of focal electrographic abnormalities). One patient reported a left-sided thunderclap headache that was stabbing in quality and lasted 30 s without recurrence or associated neurological symptoms. Headaches generally resolved in less than a day.

Movement symptoms: tremor/asterixis/myoclonus

Thirty-nine patients had tremor, asterixis, myoclonus, or some combination. The most common movement symptom was a heightened physiological tremor, which was appreciated in 28 patients and was typically mild and resolved without treatment. Thirteen patients developed a more disabling tremor, characterized by a higher amplitude and variable association with rest, intention, or postural movements. One patient developed a severe facial and tongue tremor requiring total parenteral nutrition. Asterixis was observed in eight patients, and frank myoclonus was observed in three patients. Of note, tremor and asterixis were often the earliest signs of neurotoxicity to develop after infusion, presenting within the first 5 days after infusion in 23 cases; in two patients tremor appeared on the day of infusion.

Autonomic instability

Two patients developed autonomic instability, manifesting predominately as severe postural orthostatic hypotension. In both cases, patients required prolonged treatment with midodrine, fludrocortisone, and an abdominal binder. Six other patients experienced isolated episodes of orthostatic hypotension.

Death

Five patients died after receiving CAR T cells; only one death was directly related to neurotoxicity. This patient, a 21-year-old male treated for relapsed B-cell acute lymphoblastic leukaemia, developed acute obtundation progressing to coma and brain death on post-transfusion Day 5 (Torre *et al.*, 2018). On head CT, he was found to have diffuse cerebral oedema (Supplementary Figs 1 and 2A–D). The other patients all died from disease progression or CRS: one patient died from disease progression (mantle cell lymphoma) 2 months after CAR T transfusion; another died from disease progression from chronic lymphocytic leukaemia transformed to non-Hodgkin's lymphoma 6 weeks after undergoing CAR T-cell transfusion; a third patient died 7 days after CAR T-cell transfusion from multisystem organ failure in the setting of severe CRS and infection; and a fourth patient died 12 days after CAR T-cell transfusion from multi-system organ failure in the setting of progressive diffuse large B cell lymphoma following grade 4 CRS (Fig. 2E–H).

Focal neurological symptoms

Aphasia

Aphasia was noted in 35 cases. Aphasic patients were described clinically as having 'decreased fluency', 'diminished

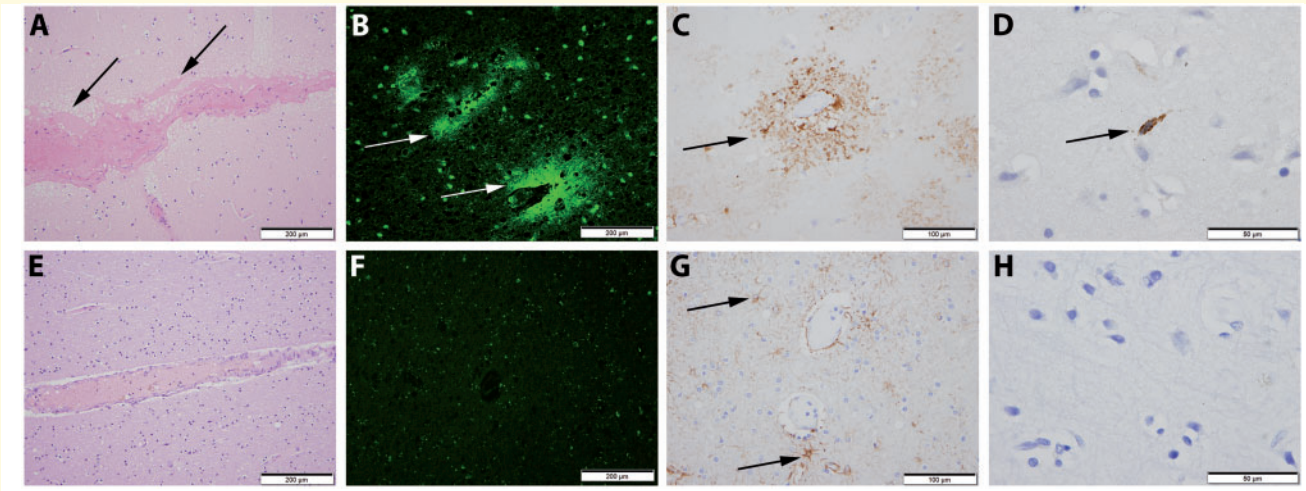

Figure 2 Neuropathology from two patients who died in the setting of severe toxicity. Microscopic evaluation of the brain of the patient with CTCAE grade 5 neurotoxicity and diffuse cerebral oedema was notable for perivascular extravasation of an acellular proteinaceous substance (**A**, arrows; haematoxylin and eosin) that stained positive for fibrin (**B**, arrows; fibrin immunofluorescence); there was marked clasmatodendrosis, particularly around vessels (**C**, arrow; GFAP immunohistochemistry), suggestive of blood–brain barrier dysfunction. Increased activated rod microglia were present (**D**, arrow; CD68 immunohistochemistry). In contrast, microscopic evaluation of the brain of the patient who died from disease progression after grade 4 CRS but without history of neurotoxicity was negative for perivascular fibrin extravasation (**E**, haematoxylin and eosin; **F**, fibrin immunofluorescence); scattered astrocytes were present by vessels (**G**, arrows; GFAP immunohistochemistry), but there was no clasmatodendrosis. Activated rod microglia were not identified (**H**; CD68 immunohistochemistry).

fluency', or 'word-finding difficulty'. In more severe cases patients experienced 'broken speech' limited to one to two word phrases, and had difficulty with naming or following commands. In six cases aphasia was so severe that the patients became globally aphasic (i.e. mute). Although the onset and progression were typically insidious over hours to days, language symptoms were sometimes abrupt in onset, mimicking acute ischaemic stroke (and on one occasion led to activation of the inpatient stroke team). In all cases aphasia symptoms resolved completely by the time of discharge.

Of the 35 patients who developed aphasia, nearly all (34/35) also had symptoms of encephalopathy. Symptoms of delirium and aphasia often occurred together in a predictable, stepwise progression. Mild dysfluency and/or word finding difficulty appeared first, accompanied by mild confusion or disorientation; in the subset that developed more severe language deficits, symptoms then progressed towards more dense aphasias and in extreme cases mutism, accompanied by an abulic or catatonic-like mental state. Interestingly, in all cases of severe aphasia, following the resolution of language symptoms patients were amnestic to the experience.

Focal weakness

Eleven patients developed focal weakness, which was transient in all but one case. In one case, left-sided weakness occurred in the setting of an acute embolic stroke (described below); these symptoms improved rapidly and resolved completely within a day. Another patient developed acute onset right-sided hemiplegia and aphasia. STAT CT with CT angiography revealed no acute intracranial pathology, MRI brain was negative for stroke, and EEG showed only left-sided slowing with no seizures. Symptoms gradually improved over days and the patient's neurological function returned to baseline 9 days after symptom onset. A third patient experienced several days of fluctuating right arm and leg weakness in the setting of aphasia that improved by discharge. Another patient had 1 day of right-sided pronator drift in the setting of aphasia. Mild non-disabling unilateral facial weakness was noted in three patients, left face and arm weakness in another, and in one patient bilateral proximal lower extremity weakness was observed. One patient had guttural and lingual dysarthria that worsened and then resolved over the course of 3 weeks. One patient had severe and prolonged quadriparesis in the setting of grade 4 CRS and grade 4 neurotoxicity; EMG/nerve conduction study was performed and the patient was diagnosed with critical illness myopathy. Over the course of a prolonged hospitalization lasting >2 months she slowly began to regain strength in her limbs.

Vision changes

Seven patients reported vision changes that were transient and mild; in no cases were persistent visual field deficits or decreased acuity experienced. One patient reported blurry vision starting 8 days after CAR T infusion, described initially as worse at distance compared to near vision. Over subsequent days the blurriness resolved but the patient reported a 'shimmering' sensation when he closed his eyes. Given concurrent headache, negative long-term monitoring

EEG, and normal ophthalmological exam this symptom was ascribed to migraine. Another patient developed dark floaters in her right eye 14 days after CAR T infusion. Ophthalmological exam revealed no acute pathology, and symptoms resolved after discharge. Another patient reported scintillating scotoma after CAR T-cell infusion without headache. A fourth patient experienced an episode of visual loss lasting 10 min accompanied by slowly migrating sensory changes and culminating in headache; long-term monitoring EEG later demonstrated an evolving pattern of lateralized rhythmic delta concerning for possible seizure. Given the absence of temporal correlation with symptoms and focal hypometabolism on PET imaging (described in greater detail below), the precise aetiology of this event (seizure versus migrainous phenomenon) remained uncertain. Another patient reported a transient episode of seeing 'squiggly lines' and 'dark spots' in the setting of a headache. Two patients reported complex formed visual hallucinations in the setting of encephalopathy.

Seizure

Seizures were uncommon; only one patient experienced an unambiguous clinical convulsion—he suffered a 45-s generalized tonic clonic seizure 8 days after CAR T-cell infusion. CT, CT angiography, MRI, and transcranial Doppler ultrasound were negative for acute pathology. EEG was not recorded during the event, and subsequent long-term monitoring EEG revealed only diffuse polymorphic theta/delta slowing with periods of rhythmic slowing and occasional bilateral independent periodic discharges. In another patient who reported vision changes and migratory sensory changes (mentioned in the paragraph above), long-term monitoring EEG demonstrated prolonged runs of evolving lateralized rhythmic delta on the ictal-interictal continuum concerning for possible electrographic seizure; both the electrographic findings and neurological dysfunction resolved in a few days.

Allodynia

Allodynia was observed in three cases. One patient developed paraesthesias and reported extreme sensitivity to touch over the back and trunk lasting ~3 days. Another patient had diffuse allodynia lasting 3 days in the setting of chronic patchy sensory disturbances second to underlying lymphoma. A third patient had 2 days of allodynia confined to the scalp and right hemibody.

Apraxia

Three patients developed ideamotor apraxia, discovered in all cases in the setting of using the telephone. One patient, on post-infusion Day 2, noted difficulty using her telephone. On exam, she was unable to simulate lighting a cigarette despite having smoked for several years. Her language was intact and she had full strength in all extremities. Symptoms resolved after 2 days. Another patient also developed significant difficulty using her telephone, and on exam could not demonstrate how to brush her teeth. A third patient was noted to struggle with his telephone; on exam, he had difficulty following complex commands but had no other symptoms of neurotoxicity.

Structural neurological injuries

Stroke

Ischaemic stroke was observed in two patients. In one patient with a history of hypertension, hyperlipidaemia, diabetes mellitus type 2, and prior tobacco use, a small embolic-appearing infarct was found in the left temporal lobe on an MRI obtained on post-treatment Day 8 for evaluation of encephalopathy (Fig. 3A). Serum CRP had peaked at 228 mg/l 2 days prior to the discovery of the infarct. A second patient with a history of hypertension, hyperlipidaemia, coronary artery disease, and atrial fibrillation (not being treated with anticoagulation because of thrombocytopaenia) who had ongoing fluctuating encephalopathy developed acute left-sided weakness on post-treatment Day 13; MRI demonstrated acute embolic appearing infarcts in multiple vascular territories (Fig. 3B). Focal weakness rapidly resolved without acute intervention. Laboratory evaluation in this case was significant for a platelet count of 22 K/μl, an elevated prothrombin time of 16.4 s (international normalized ratio of 1.4), and a depressed serum fibrinogen of 178 mg/dl, concerning for disseminated intravascular coagulation. A third patient with a history of hypertension developed isolated acute aphasia 22 days post-CAR T transfusion. Symptoms resolved completely within hours of onset, and MRI was negative for acute ischaemia. The event was felt by the consulting neurologist to most likely represent transient ischaemic attack rather than CAR T-cell-associated neurotoxicity.

Intracranial haemorrhage

Two patients suffered spontaneous subarachnoid haemorrhage. One patient had a head CT in the setting of worsening confusion on post-infusion Day 13 that revealed a Fisher grade 2 subarachnoid haemorrhage in the setting of profound thrombocytopaenia (platelet count 19 K/μl) (Fig. 3C). No aneurysm or other vascular malformation was identified. The other patient was found to have scattered subarachnoid haemorrhage over the right cerebral convexity on head CT obtained in the setting of encephalopathy (Fig. 3D). No clear vascular source could be identified. A patient with multiple myeloma presented 9 days after treatment with CAR T cells with vertigo; over subsequent weeks she developed rapidly progressive bilateral sensorineural hearing loss and was ultimately discovered on MRI to have bilateral intralabyrinthine cochlear haemorrhages. The treating oncology team and haematology consult service felt this was a direct sequelae of her underlying myeloma rather than CAR T-cell treatment.

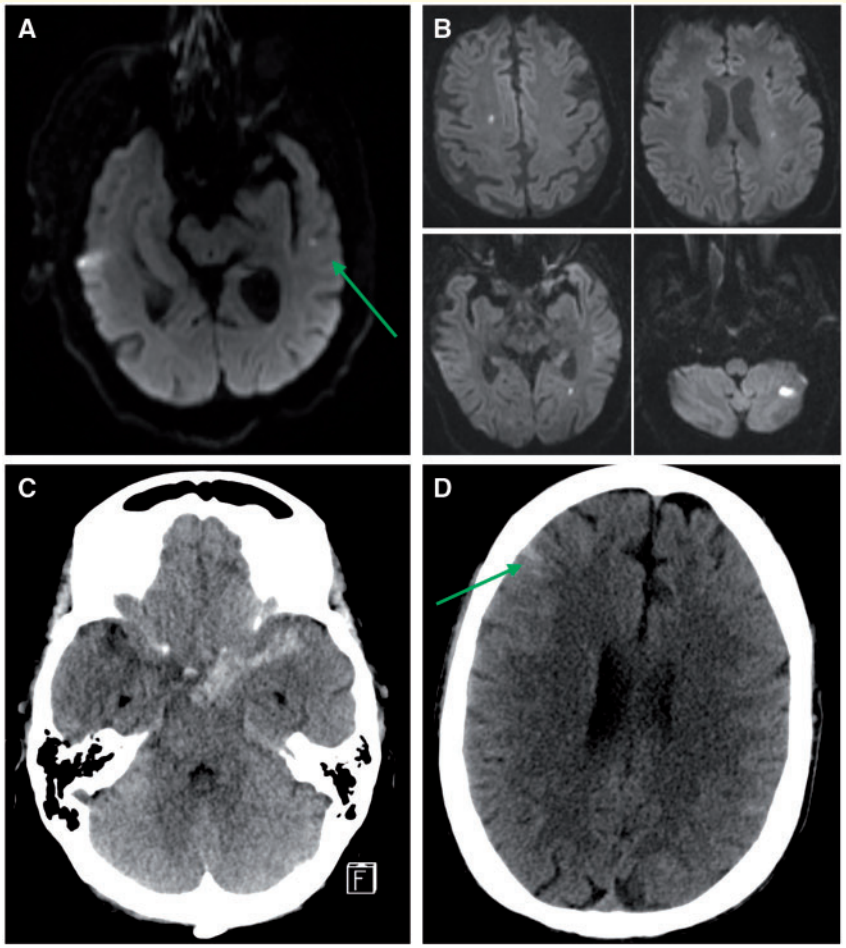

Figure 3 Four cerebrovascular injuries that occurred during CAR T-cell therapy. (**A**) Acute ischaemic stroke in the left temporal lobe in a patient with generalized encephalopathy. (**B**) Scattered foci of restricted diffusion in multiple vascular territories, suggestive of a central embolic event, in a patient with encephalopathy that developed acute left-sided weakness. (**C**) Non-aneurysmal subarachnoid haemorrhage in the left Sylvian fissure in a patient with profound thrombocytopenia that developed worsening confusion and transient aphasia. (**D**) Trace convexity subarachnoid haemorrhage in a patient with progressive obtundation and respiratory failure resulting in intubation.

Diagnostic studies

Conventional neuroimaging: CT and MRI

Non-contrast head CT was the most commonly obtained neurodiagnostic study. Ninety-nine CT scans were obtained in 48 patients. Four abnormal findings were noted: the two cases of subarachnoid haemorrhage, one of the two ischaemic strokes, and the case of diffuse cerebral oedema described above. MRI was obtained in 29 cases. The only acute intracranial findings noted on MRI were two cases of ischaemic stroke, two cases of subarachnoid haemorrhage, and the case of bilateral intralabyrinthine cochlear haemorrhages described previously.

Twenty-six patients underwent either CT angiography or magnetic resonance angiography. In 22 cases, CT angiography/magnetic resonance angiography was either normal or demonstrated only mild atherosclerotic disease. In four cases, more unusual focal vessel abnormalities were noted. In one case, a patient with prolonged encephalopathy initially had an unremarkable CT angiography, but on magnetic resonance angiography obtained 2 weeks later, mild narrowing of the right anterior cerebral artery (ACA) concerning for vasospasm was noted. In a second case, moderate to severe bilateral focal ACA narrowing was noted in a patient with neurotoxicity-associated encephalopathy and aphasia. CT angiography in a third patient with mild confusion and language dysfunction also demonstrated diffuse irregularity of the intracranial and vertebral arteries. A fourth patient who had both encephalopathy and spontaneous subarachnoid haemorrhage on imaging underwent magnetic resonance angiography that demonstrated focal areas of narrowing within the middle cerebral artery (MCA) branches; a follow-up scan at 2 weeks showed improvement but not complete resolution.

EEG

Thirty-six patients with neurotoxicity underwent EEG. In 28 cases, the background was notable for generalized

slowing in the theta-delta range. Of those patients with slowing, the majority (17/28) had a loss of the posterior dominant rhythm, though almost all (23/28) had preservation of the antero-posterior gradient. Several other non-epileptiform EEG abnormalities were also noted, including generalized asynchronous slow activity (2/36) and focal slowing (12/36), in some cases with accompanying focal attenuation (3/12). Patients with focal EEG abnormalities often had focal neurological symptoms including aphasia (9/12), scotoma (1/12), and focal weakness (1/12).

Rhythmic activity was seen in 19 of 36 patients. The most common rhythmic pattern was frontally predominant generalized rhythmic delta activity (RDA) (14/19), typically in the 0.5–2.5 Hz range. Several patients exhibited more concerning activity on ictal-interictal continuum including lateralized rhythmic delta activity (2/19) and generalized periodic discharges (9/19). All generalized periodic discharges were noted, at times, to have triphasic morphology. A few patients exhibited sporadic discharges, including spike-wave discharges (4/36) and epileptiform discharges (3/36). One patient experienced a clinical generalized tonic-clonic seizure, and one patient had an EEG pattern in the ictal-interictal continuum concerning for possible electrographic seizure (Fig. 4A–F), though given discordant ^{18}F-fluorodeoxyglucose (FDG)-PET imaging findings (Fig. 6F) and uncertain clinical correlate the precise aetiology remained uncertain.

Transcranial Doppler ultrasound

Thirty-one patients underwent a total of 80 transcranial Doppler studies. There was no significant difference in flow velocities in any of the vascular territories as a function of neurotoxicity grade in our cohort (Fig. 5A). Interestingly, however, we did observe a significant increase in flow velocities in the patients who had clear focal neurological deficits compared to patients who had only very mild symptoms or encephalopathy without focal deficits [ACA: mean velocities 93.12 cm/s versus 65.48 cm/s, $t(73) = 6.307$, $P = 1.27 \times 10^{-6}$; MCA: mean velocities 108.20 cm/s versus 72.51 cm/s, $t(72) = 7.124$, $P = 6.534 \times 10^{-10}$, posterior cerebral artery (PCA): mean velocities 64.35 cm/s versus 47.08 cm/s, $t(68) = 5.323$, $P = 1.95 \times 10^{-4}$; unpaired two-sample two-tailed Student's *t*-tests] (Fig. 5B). Among the 28 patients who underwent both transcranial Doppler ultrasound and EEG, we noted similar differences in flow velocities between patients who had focal or lateralized EEG abnormalities versus only generalized EEG findings, with statistically significant greater mean velocities in the ACA and MCA and a trend toward higher mean velocities in the posterior cerebral artery in patients with focal/lateralized findings [ACA: mean velocities 86.25 cm/s versus 69.13 cm/s, $t(26) = 2.099$, $P = 0.0457$; MCA: mean velocities 102.8 cm/s versus 77.38 cm/s, $t(26) = 2.4$, $P = 0.0238$, PCA: mean velocities 59.08 cm/s versus 45.4 cm/s, $t(25) = 1.886$, $P = 0.0710$; unpaired two-sample two-tailed Student's *t*-tests].

FDG-PET

Six patients who developed neurotoxicity and had abnormal EEGs underwent FDG-PET scans of the brain. In one case, EEG was notable for left hemispheric attenuation, loss of higher frequencies, and hemispheric slowing in addition to frontally predominant generalized RDA (Fig. 6A). FDG-PET showed an asymmetric decrease in tracer uptake in the left frontal lobe, caudate, and right cerebellum (Fig. 6B). In another patient, EEG was notable for intermittent generalized sharply-contoured semi-rhythmic activity (Fig. 6C). FDG-PET was notable for diffuse cortical hypometabolism involving bilateral frontal, temporal, and parietal lobes with sparing of the sensorimotor cortices bilaterally and occipital lobes. Hypometabolism was also noted in the posterior cingulate gyrus (Fig. 6D). Another patient, who was previously mentioned, had an EEG that at times had ictal-appearing runs of right-sided RDA (Fig. 6E). FDG-PET showed hypometabolism in the posterior-lateral right temporal lobe and right parietal lobe (Fig. 6F). In a fourth patient, EEG was notable for generalized theta-delta slowing with shifting predominance. Early in his course EEG was also notable for intermittent generalized RDA (Fig. 6G). FDG-PET showed bilateral, right greater than left frontal lobe and right temporal lobe hypometabolism (Fig. 6H). A fifth patient with encephalopathy and aphasia had an EEG that revealed bilateral slowing and generalized RDA (Fig. 6I). FDG-PET showed global hypometabolism in the cortical grey matter (Fig. 6J). In the sixth case, EEG demonstrated generalized theta/delta slowing, and FDG-PET demonstrated global hypometabolism.

Interestingly, in three of these cases, transcranial Doppler ultrasound demonstrated elevated flow velocities in the regions of FDG-PET hypometabolism. In the case illustrated in Fig. 6B, transcranial Doppler ultrasound revealed elevated velocities in the left MCA (peak mean flow velocity 112 cm/s). In the case illustrated in Fig 6D, flow velocities were elevated in the bilateral MCAs (peak mean flow velocity 119 cm/s in the left MCA and 109 cm/s in the right MCA). In the case illustrated in Fig. 6F, transcranial Doppler ultrasound showed elevated velocity in the right ACA (peak mean flow velocity 110 cm/s) and right PCA (peak mean flow velocity 90 cm/s).

Lumbar puncture

Thirteen patients underwent lumbar puncture. One additional patient who had an external ventricular drain placed for intracranial pressure monitoring also had CSF sampled for analysis. In most cases CSF was either non-inflammatory or minimally inflammatory (median white blood cells in tube #1 was 3/μl, range 0–35; median protein 51.0 mg/dl, range 27.1 – 234.3). There were $\leqslant 5$ white blood cells/μl in all but five cases and CSF protein was < 60 mg/dl in all but three cases (Table 2). CSF culture was negative for bacterial growth in the 11 instances it was sent, and CSF cytology was negative for malignancy in eight of the nine instances it was performed.

Neuropathology

Post-mortem examination was performed on two patients. The first patient, a 21-year-old male with relapsed acute

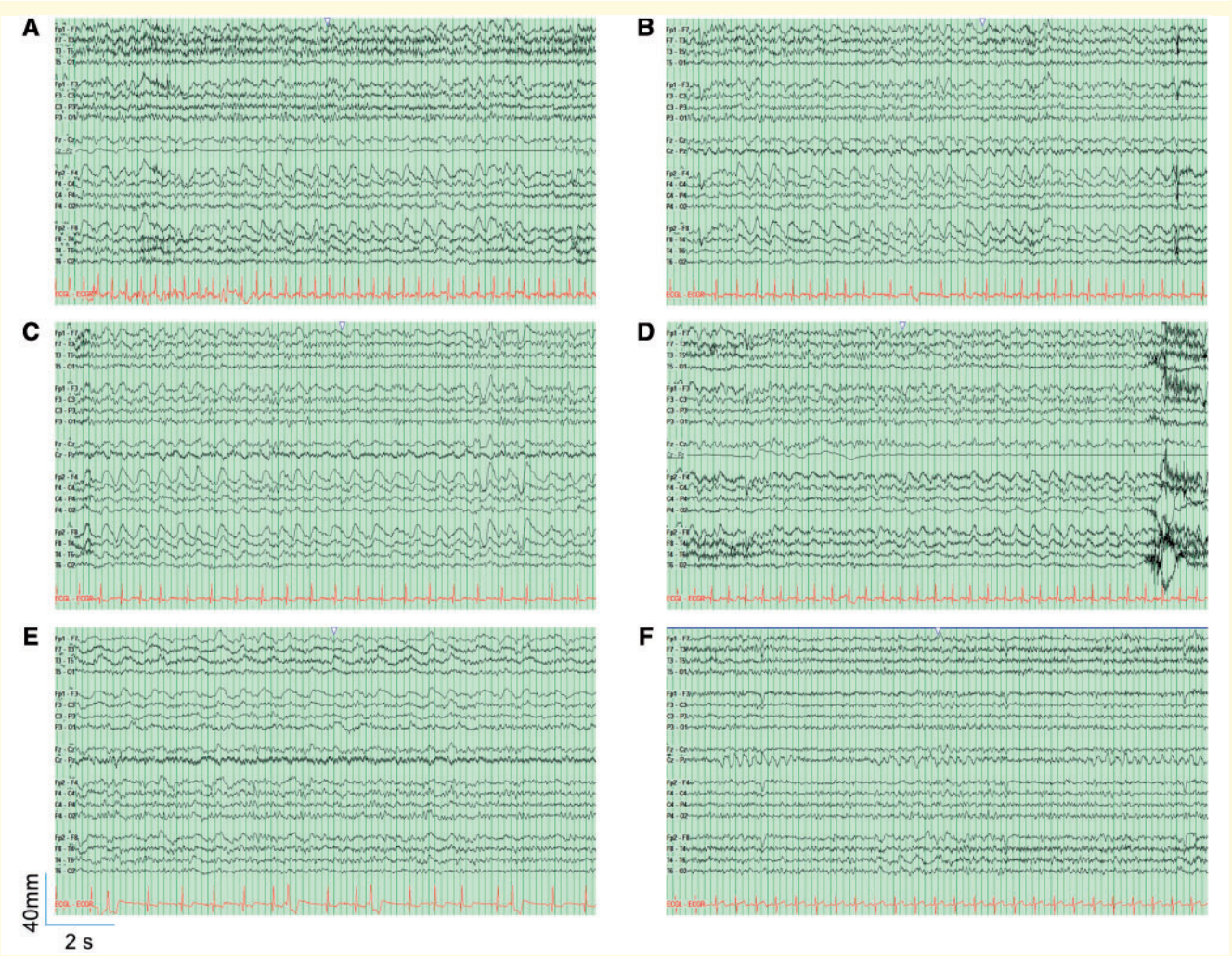

Figure 4 Temporal evolution of EEG in a patient with CAR-T-induced neurotoxicity. (**A**–**F**) Longitudinal bipolar montage (left-left-midline-right-right-ECG), sensitivity 7 μV/mm, time base 30 mm/s, low frequency filter 1 Hz, high frequency filter 70 Hz, notch 60 Hz. Scale is provided with *y*-axis representing voltage amplitude (μV) and the *x*-axis representing time (s). (**A**) The EEG on Day 1 was notable for a poorly organized background predominantly in the theta range, with intermittent runs of right frontal RDA, 2.0–2.5 Hz, with (**B**) spread to the posterior as well as (**C**) contralateral leads, lasting for 30–40 min. (**D**) At least one of these runs satisfied the modified Young's criteria (Young *et al.*, 1996; Hirsch *et al.*, 2005) for an electrographic seizure. During this time, exam was notable for intact fluency and comprehension, an intermittent left visual field deficit, and patchy sensory disturbance over left arm. (**E**) On Day 2 the lateralized RDA became left frontal predominant at onset, at which time the patient was noted to have confusion, inability to follow commands, incomprehensible speech and word finding difficulties. (**F**) On Day 5, EEG was notable for right greater than left temporal slowing, and the patient reported an episode of marching numbness that spread from his left hand, up to his shoulder and eventually to the face. The episode was associated with a visual scotoma but no headache. FDG-PET showed hypometabolism in the posterior-lateral right temporal lobe and right parietal lobe (Fig. 6F).

lymphoblastic leukaemia who developed CTCAE grade 5 neurotoxicity, had a markedly oedematous brain (weight 1680 g, normal range 1250–1400 g) with flattened gyri and compressed sulci and ventricles. Microscopically, the brain showed expansion of the perivascular spaces, which were frequently occupied by an acellular eosinophilic material (Fig. 2A) that was positive for fibrin by immunofluorescence studies (Fig. 2B). In addition, there was severe astrocyte injury, as evidenced by widespread clasmatodendrosis—a beading and fragmentation of astrocytic processes [highlighted by glial fibrillary acidic protein (GFAP)]. Clasmatodendrosis was particularly prominent around vessels (Fig. 2C), suggestive of blood–brain barrier dysfunction. Activated rod microglia (highlighted by CD68) were also present (Fig. 2D). Notably, there was no evidence of CAR T cell or exuberant reactive lymphoid infiltrate, involvement by leukaemia cells, or infection. The second patient, a 55-year-old male with relapsed/progressive diffuse large B cell lymphoma and no history of neurotoxicity following CAR T-cell infusion who died from disease progression following severe CRS, had an externally unremarkable brain (weight 1570 g) without significant

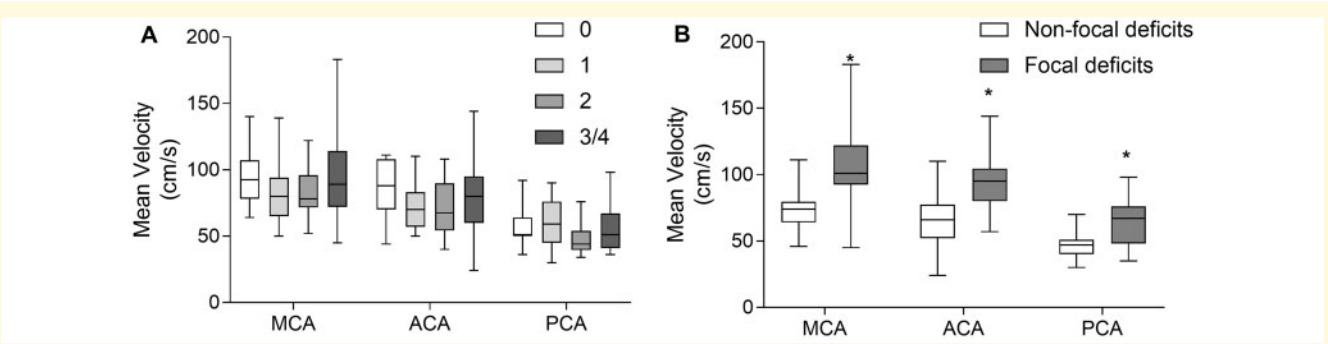

Figure 5 Transcranial Doppler reveals increased flow velocity in many patients with CAR T-induced neurotoxicity: (**A**) No significant relationship was observed between flow velocity and neurotoxicity grade. (**B**) Patients with focal neurological deficits as opposed to non-localizing neurological symptoms had significantly greater flow velocities in all vessels. See main text for details. Box (whiskers) shows median ± 1.0 IQR (minimum to maximum).

oedema. Microscopically, the brain was also unremarkable. Perivascular fibrin extravasation was not identified (Fig. 2E-F), and there was no clasmatodendrosis (Fig. 2G), atypical lymphoid infiltrate, increased activated microglia (Fig. 2H), or evidence of infection.

Discussion

Neurotoxicity is common in CAR T-cell therapy. At BWH/DFCI, patients undergoing CAR T-cell therapy requiring intensive care unit-level care are triaged to neuro-intensive care unit, emphasizing the primacy of neurotoxicity in this treatment modality. In our cohort, at least one symptom of neurotoxicity was observed in 77 of 100 cases (77%). The most common neurological symptoms encountered in this study were encephalopathy, aphasia, headache, and tremor, although focal weakness, vision changes, apraxia, allodynia, and dysautonomia were encountered as well. Seizure, stroke, or intracranial haemorrhage occurred in a small minority of cases. Neuroimaging studies were commonly performed for the evaluation of neurotoxicity but rarely revealed structural abnormalities. Given the common occurrence of focal neurological symptoms, the absence of structural findings, and frequent EEG, PET, and transcranial Doppler abnormalities, these data raise significant questions regarding the underlying pathophysiological mechanisms.

Comparison with previously published reports

As has been described previously, the most common neurotoxicity encountered in our cohort was encephalopathy. This is consistent with all previously published studies, which reported rates of encephalopathy ranging from 25% to 62% (Grupp *et al.*, 2013; Davila *et al.*, 2014; Maude *et al.*, 2014; Kochenderfer *et al.*, 2015; Lee *et al.*, 2015; Turtle *et al.*, 2016*a*, *b*; Gust *et al.*, 2017; Neelapu *et al.*, 2017; Schuster *et al.*, 2017; Gofshteyn *et al.*, 2018). Headache was also reported in several prior studies (Kochenderfer *et al.*, 2015; Lee *et al.*, 2015; Hu *et al.*, 2016); although given its generally benign quality, may be under-reported in the literature. Other transient neurological symptoms described herein, including aphasia, vision changes, tremor, and facial droop, have also been previously described at rates similar to those reported here (Davila *et al.*, 2014; Maude *et al.*, 2014; Kochenderfer *et al.*, 2015; Lee *et al.*, 2015; Hu *et al.*, 2016; Turtle *et al.*, 2016*b*; Gust *et al.*, 2017; Neelapu *et al.*, 2017; Schuster *et al.*, 2017; Gofshteyn *et al.*, 2018).

As in studies reported previously, standard neuroimaging with CT or MRI was generally unrevealing (Grupp *et al.*, 2013; Davila *et al.*, 2014; Maude *et al.*, 2014; Schuster *et al.*, 2017), although there are isolated reports of CT and MRI abnormalities, including a T_2 splenial lesion in one case (Lee *et al.*, 2015) and a pontine haemorrhage in another (Turtle *et al.*, 2016*b*). One case series described T_2 hyperintensities, with or without contrast enhancement, leptomeningeal enhancement, microhaemorrhages, or diffuse diffusion restriction in 7 of 23 patients imaged with MRI (Gust *et al.*, 2017). These findings were not present in any of the cases reported here; the reason for this discrepancy is unknown but may be due to differences in types of malignancies or CAR T-cell products used. Other than for ruling out acute stroke or haemorrhage (in the four cases described), CT and MRI was generally of little diagnostic value.

Pathophysiology and evaluation of neurotoxicity

The primary challenge in understanding the pathophysiology of CAR T-cell neurotoxicity lies in accounting for focal neurological symptoms, despite a general absence of structural brain lesions. Although strokes and intracranial haemorrhages occurred both within the cohort described here and in the literature, these events were rare, and unlikely to account mechanistically for most cases of neurotoxicity. For this reason, in our cohort we focused on functional diagnostic studies such as transcranial Doppler ultrasound, EEG and FDG-PET. Although no clear

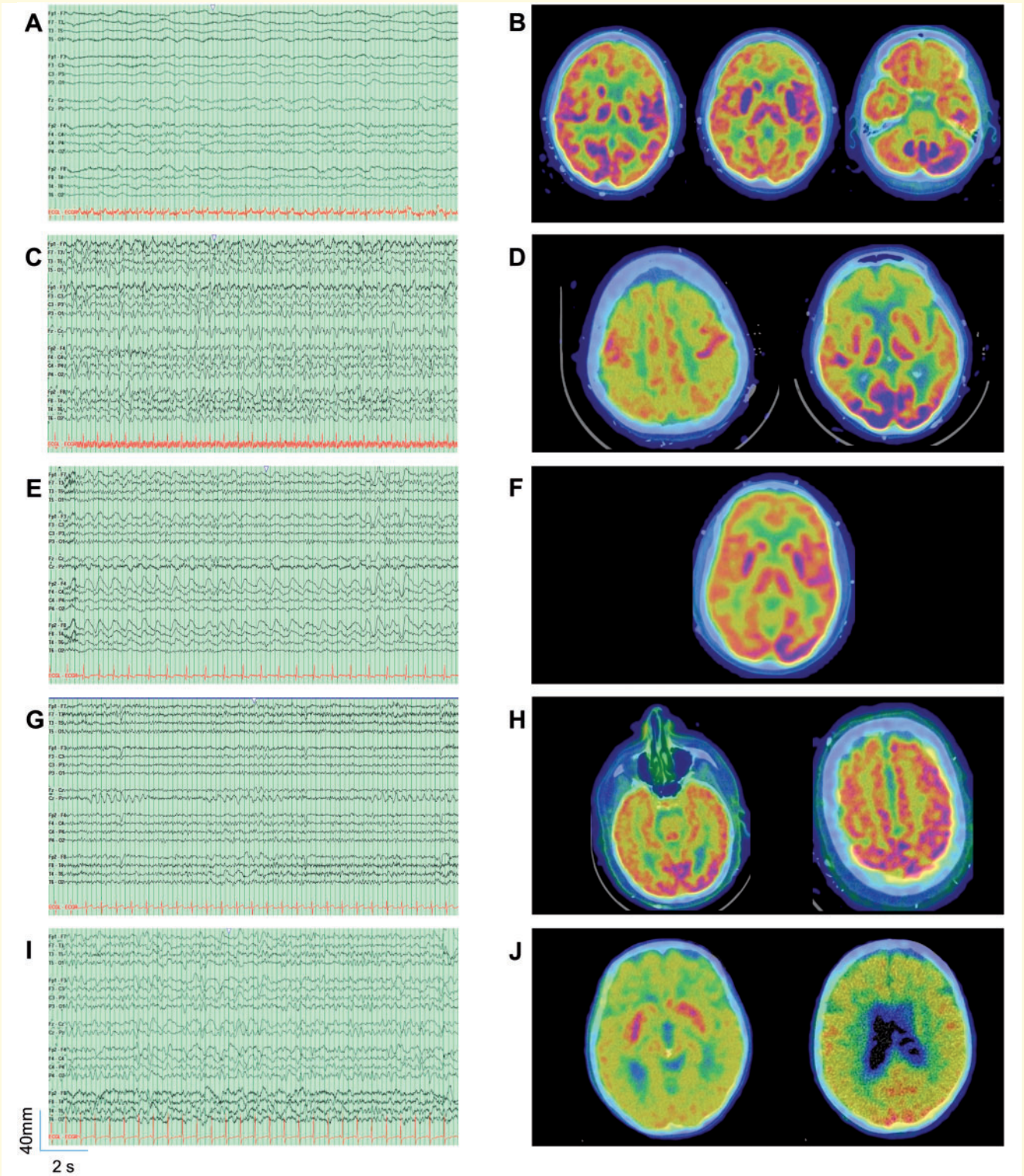

Figure 6 FDG-PET abnormalities from five clinical cases of CAR T-cell neurotoxicity: EEGs (**A**, **C**, **E**, **G** and **I**) and brain FDG-PET/CT scans (**B**, **D**, **F**, **H** and **J**) of patients with CAR T-cell-associated neurotoxicity. EEG abnormalities are associated with areas of focal hypometabolism on FDG-PET. EEGs are presented in longitudinal bipolar montage (left-left-midline-right-right-ECG), sensitivity 7 μV/mm, time base 30 mm/s, low frequency filter 1 Hz, high frequency filter 70 Hz, notch 60 Hz. Scale is provided with *y*-axis representing voltage amplitude (μV) and the *x*-axis representing time (s).

Table 2 CSF studies

WBCs, cells/μl; Tube 1, Tube 4 (if present)	Protein, mg/dl	Glucose, mg/dl	Culture	Cytology
14, 11	44.1	66	Negative	Negative
4, 0	57.2	102	Negative	Negative
13, 7	34.2	82	Negative	
1, 1	27.1	54	Negative	
1	29.8	60		Negative
4, 2	57.6	72		Negative
12, 7	51.4	46	Negative	Negative
2, 1	35.5	61	Negative	'Suspicious for malignancy'
8, 4	234.3	49	Negative	Negative
1	51.0	59		
0, 0	145.2	94	Negative	Negative
0, 0	7.1	129	Negative	
35, 20	89.7	69	Negative	Negative
0, 0	33.7	98	Negative	

WBCs = white blood cells.

relationship between transcranial Doppler flow velocities and neurotoxicity severity was observed, we did note a significant increase in overall flow velocities in patients with focal rather than global deficits. While not formally validated at this time, these findings suggest that transcranial Doppler ultrasound may become a useful adjunct biomarker for CAR T-cell-induced neurotoxicity.

While seizures were rare in our cohort, nonspecific but frequently focal EEG abnormalities were commonly observed during neurotoxicity. Prior reports have varied significantly regarding the frequency of seizure in this patient population. One trial reported seizures in 3 of 30 patients (Turtle *et al.*, 2016*a*) and in a large retrospective analysis of 133 patients, seizures were observed in four patients (Gust *et al.*, 2017). A more recent study reported seizure in 4 of 51 patients (Gofshteyn *et al.*, 2018). One trial reported 'seizure-like' activity on EEG in all six patients that developed neurotoxicity, which improved after treatment with anti-epileptic drugs, though seizures were not specifically reported in this study. Previously published reports (Gust *et al.*, 2017; Herlopian *et al.*, 2018) as well as our experience suggests that neurological toxicity is associated with rhythmic or periodic electrical activity, particularly in the ictal-interictal continuum. This represents a spectrum of neurophysiological dysfunction, the clinical significance of which is unknown (Chong and Hirsch, 2005; Osman *et al.*, 2018). FDG-PET has emerged as a method of characterizing the metabolic impact of ictal-interictal continuum patterns and serves as a means of evaluating for metabolic stress and neuronal injury (Struck *et al.*, 2016). Interestingly, in five of our cases in which patients underwent both EEG and FDG-PET, the foci of concerning activity seen on EEG was correlated with areas of hypometabolism on FDG-PET, in contrast to the hypermetabolism more commonly seen in cases of focal status epilepticus (Vespa *et al.*, 2010; Struck *et al.*, 2016). These findings taken together suggest against seizure as a common underlying mechanism of neurotoxicity.

An inflammatory process, such as an autoimmune encephalitis triggered by CAR T cells, has been implicated as a potential cause of neurotoxicity. In a recently published animal model of CAR T-cell-associated neurotoxicity, rhesus macaque monkeys with neurotoxicity were found to have elevated CSF levels of pro-inflammatory cytokines and accumulated high levels of CAR and non-CAR T cells within the both the grey and white matter of the brain parenchyma as well as the CSF (Taraseviciute *et al.*, 2018). In several published trials, CAR T cells and other inflammatory cytokines were isolated from the CSF (Grupp *et al.*, 2013; Lee *et al.*, 2015; Hu *et al.*, 2016), supporting this hypothesis. However, in at least some trials CAR T cells were just as likely to be found in the CSF of patients not experiencing neurotoxicity, and their presence or absence was not predictive of neurological symptoms (Maude *et al.*, 2014). In one case report of a patient who died from CAR T-cell-associated neurotoxicity, extensive CNS inflammation was observed on autopsy (Schuster *et al.*, 2017). However, in other case reports of fatal cerebral oedema from CAR T-cell therapy, no inflammation was noted and only astrocyte injury and proteinaceous exudate was observed (Torre *et al.*, 2018). Furthermore, within our patient population, evidence of CNS inflammation was rare; most patients who underwent lumbar puncture had bland CSF. Thus, it is not clear if CNS inflammation is truly pathophysiological or rather an epiphenomenon of CAR T-cell therapy and/or concurrent CRS.

Diffuse cerebral oedema has been described as one of the more devastating sequelae of CAR T-cell neurotoxicity (Hu *et al.*, 2016; Gust *et al.*, 2017; Schuster *et al.*, 2017). However, we observed only one case of clinically significant cerebral oedema in our cohort (Torre *et al.*, 2018),

and though oedema itself may arise as the sequelae of some other underlying process, it is unlikely to be the main cause of neurological symptoms in this cohort and failed to demonstrate any active inflammation.

An alternative explanation is that neurotoxicity occurs as the result of widespread endothelial activation and subsequent increased permeability of the blood–brain barrier (Gust *et al.*, 2017; Norelli *et al.*, 2018; Santomasso *et al.*, 2018). This provides a potential mechanism for the cases of diffuse and often fatal cerebral oedema that have been reported in multiple cohorts (including our own), and is supported by findings of widespread endothethial activation and disruption from pathological specimens in humans that died from CAR T-cell-associated neurotoxicty (Gust *et al.*, 2017) as well as findings of meningeal inflammation and blood brain barrier breakdown from a mouse model of CAR T-cell neurotoxicity (Norelli *et al.*, 2018). CRS-promoted endothelial dysfunction is also supported by clinical trials demonstrating elevated levels of pro-inflammatory cytokines in patients who experience neurotoxicity (Turtle *et al.*, 2016*a*, *b*, 2017), and the finding both in our cohort and previously published trials that neurotoxicity often occurs several days after the peak of CRS (Turtle *et al.*, 2016*a*; Gust *et al.*, 2017). Regional endothelial dysfunction causing focal neurological deficits and even seizures has been implicated in other disease states such as eclampsia or posterior reversible encephalopathy syndrome (Hinchey *et al.*, 1996; Feske and Singhal, 2014). Increased blood–brain barrier permeability may disrupt the local homeostasis of extracellular contents resulting in cortical circuit dysfunction, such as cortical spreading depression. Such a mechanism could account for periods of both focal and generalized symptoms, the lack of structural findings on imaging, the absence of impressive signs of CNS inflammation, the non-specific EEG slowing observed, cortical hypometabolism on seen on FDG-PET, and the reversibility of symptoms.

In terms of predicting the time course and severity of neurotoxicity, several findings from this cohort study bear highlighting. Although symptoms could present at virtually any time within the first few weeks after CAR T-cell infusion, in our experience patients who developed early CRS were more likely to develop neurotoxicity and were more likely to develop severe neurotoxicity. These patients likely warrant closer monitoring and early and more aggressive toxicity-directed treatment. Additionally, most of the neurotoxicity observed in this cohort was in the 84 treatments administered for leukaemia or lymphoma; the 14 cases treated for myeloma and two patients treated for sarcoma had minimal neurotoxicity, and in cases where it did occur, it was generally attributable to other causes (e.g. confusion noted in a patient with sepsis and multi-system organ failure from gram negative bacteraemia). It is uncertain from these data whether these observations are due to true differences in the likelihood of toxicity based on underlying disease or are a consequence of the different CAR T-cell constructs. Different CAR T-cell molecular targets, dosing regimens, conditioning protocols, and concurrently administered targeted therapies all may influence the severity and mode of neurotoxicity encountered; however, this cohort was not powered to detect these other possible differences. Ongoing clinical trials and post-marketing surveillance will be critical in understanding these and other influences on toxicity.

The management of neurotoxicity remains an area of active investigation. Presently, corticosteroids and tocilizumab are the mainstays of treatment for both CRS and neurotoxicity (Neelapu *et al.*, 2018). Treatment with tocilizumab for CRS causes serum IL-6 to rise (Santomasso *et al.*, 2018), which may predispose to more severe neurotoxicity. This suggests that patients with even minor neurological symptoms should be treated for CRS with both tocilizumab and steroids to prevent worsening neurotoxicity. Unlike the IL-6-receptor antagonist tocilizumab, the direct IL-6 antagonist siltuximab may mitigate the toxicities associated with IL-6 without causing a rise in serum levels of IL-6 (Chen *et al.*, 2016), and could be considered as an alternative steroid-sparing therapy for patients with both CRS and neurotoxicity. Lastly, it is important to recognize that patients undergoing treatment with CAR T-cell therapy are not immune to other neurological injuries. It is thus imperative that clinicians remain vigilant in their workup and management of all neurological symptoms, especially those that deviate from the expected course of recovery and responsiveness to standard interventions.

Conclusion

Given its ability to achieve high rates of lasting remission in patients with relapsed and refractory malignancy, CAR T-cell therapy promises to transform the treatment of malignancy. One of the greatest challenges to more widespread utilization of this mode of treatment, however, will be overcoming the significant associated toxicity. By better defining the scope of the neurotoxicity encountered in this large patient population, and shedding light on some of the potential underlying pathophysiological mechanisms, we can help both clinicians and investigators to recognize, treat, and improve the care we provide to this vulnerable patient population.

Acknowledgements

The authors wish to thank Dr Allan H. Ropper, Dr Steven K. Feske, and Dr Matthew B. Bevers for helpful discussions and feedback during the preparation of the manuscript.

Funding

No funding was received towards this work.

Competing interests

C.A.J. reports consulting for Kite, Novartis, Precision Biosciences, Humanigen, Pfizer, Bayer, and Celgene. J.W.L. reports contract work with SleepMed/DigiTrace and Advance Medical, he is an officer in the American Clinical Neurophysiology Society, and chairperson of the Critical Care EEG Monitoring Research Consortium. All other authors report no conflicts of interest or competing financial interests.

Supplementary material

Supplementary material is availabnle at *Brain* online.

References

Brudno JN, Kochenderfer JN. Chimeric antigen receptor T-cell therapies for lymphoma. Nat Rev Clin Oncol 2018; 15: 31–46.

Chen F, Teachey DT, Pequignot E, Frey N, Porter D, Maude SL, et al. Measuring IL-6 and sIL-6R in serum from patients treated with tocilizumab and/or siltuximab following CAR T cell therapy. J Immunol Methods 2016; 434: 1–8.

Chong DJ, Hirsch LJ. Which EEG patterns warrant treatment in the critically ill? Reviewing the evidence for treatment of periodic epileptiform discharges and related patterns. J Clin Neurophysiol 2005; 22: 79–91.

Davila ML, Riviere I, Wang X, Bartido S, Park J, Curran K, et al. Efficacy and toxicity management of 19–28z CAR T cell therapy in B cell acute lymphoblastic leukemia. Sci Transl Med 2014; 6: 224ra25.

Feske SK, Singhal AB. Cerebrovascular disorders complicating pregnancy. Continuum (Minneap Minn) 2014; 20: 80–99.

Gofshteyn JS, Shaw PA, Teachey DT, Grupp SA, Maude S, Banwell B, et al. Neurotoxicity after CTL019 in a pediatric and young adult cohort. Ann Neurol 2018; 84: 537–46.

Grupp SA, Kalos M, Barrett D, Aplenc R, Porter DL, Rheingold SR, et al. Chimeric antigen receptor-modified T cells for acute lymphoid leukemia. N Engl J Med 2013; 368: 1509–18.

Gust J, Hay KA, Hanafi LA, Li D, Myerson D, Gonzalez-Cuyar LF, et al. Endothelial activation and blood-brain barrier disruption in neurotoxicity after adoptive immunotherapy with CD19 CAR-T cells. Cancer Discov 2017; 7: 1404–19.

Gutierrez C, McEvoy C, Mead E, Stephens RS, Munshi L, Detsky ME, et al. Management of the critically ill adult chimeric antigen receptor-T cell therapy patient: a critical care perspective. Crit Care Med 2018; 46: 1402–10.

Herlopian A, Dietrich J, Abramson JS, Cole AJ, Westover MB. EEG findings in CAR T-cell therapy-related encephalopathy. Neurology 2018; 91: 227–9.

Hinchey J, Chaves C, Appignani B, Breen J, Pao L, Wang A, et al. A reversible posterior leukoencephalopathy syndrome. N Engl J Med 1996; 334: 494–500.

Hirsch LJ, Brenner RP, Drislane FW, So E, Kaplan PW, Jordan KG, et al. The ACNS subcommittee on research terminology for continuous EEG monitoring: proposed standardized terminology for rhythmic and periodic EEG patterns encountered in critically ill patients. J Clin Neurophysiol 2005; 22: 128–35.

Hu Y, Sun J, Wu Z, Yu J, Cui Q, Pu C, et al. Predominant cerebral cytokine release syndrome in CD19-directed chimeric antigen receptor-modified T cell therapy. J Hematol Oncol 2016; 9: 70.

Kochenderfer JN, Dudley ME, Kassim SH, Somerville RP, Carpenter RO, Stetler-Stevenson M, et al. Chemotherapy-refractory diffuse large B-cell lymphoma and indolent B-cell malignancies can be effectively treated with autologous T cells expressing an anti-CD19 chimeric antigen receptor. J Clin Oncol 2015; 33: 540–9.

Lee DW, Gardner R, Porter DL, Louis CU, Ahmed N, Jensen M, et al. Current concepts in the diagnosis and management of cytokine release syndrome. Blood 2014; 124: 188–95.

Lee DW, Kochenderfer JN, Stetler-Stevenson M, Cui YK, Delbrook C, Feldman SA, et al. T cells expressing CD19 chimeric antigen receptors for acute lymphoblastic leukaemia in children and young adults: a phase 1 dose-escalation trial. Lancet 2015; 385: 517–28.

Maude SL, Frey N, Shaw PA, Aplenc R, Barrett DM, Bunin NJ, et al. Chimeric antigen receptor T cells for sustained remissions in leukemia. N Engl J Med 2014; 371: 1507–17.

Neelapu SS, Locke FL, Bartlett NL, Lekakis LJ, Miklos DB, Jacobson CA, et al. Axicabtagene ciloleucel CAR T-cell therapy in refractory large B-cell lymphoma. N Engl J Med 2017; 377: 2531–44.

Neelapu SS, Tummala S, Kebriaei P, Wierda W, Gutierrez C, Locke FL, et al. Chimeric antigen receptor T-cell therapy—assessment and management of toxicities. Nat Rev Clin Oncol 2018; 15: 47–62.

Norelli M, Camisa B, Barbiera G, Falcone L, Purevdorj A, Genua M, et al. Monocyte-derived IL-1 and IL-6 are differentially required for cytokine-release syndrome and neurotoxicity due to CAR T cells. Nat Med 2018; 24: 739–48.

Osman GM, Araujo DF, Maciel CB. Ictal interictal continuum patterns. Curr Treat Options Neurol 2018; 20: 15.

R Core Team. R: a language and environment for statistical computing. Vienna, Austria: R Foundation for Statistical Computing; 2017.

Santomasso BD, Park JH, Salloum D, Riviere I, Flynn J, Mead E, et al. Clinical and biological correlates of neurotoxicity associated with CAR T-cell therapy in patients with B-cell acute lymphoblastic leukemia. Cancer Discov 2018; 8: 958–71.

Schuster SJ, Svoboda J, Chong EA, Nasta SD, Mato AR, Anak O, et al. Chimeric antigen receptor T cells in refractory B-cell lymphomas. N Engl J Med 2017; 377: 2545–54.

Struck AF, Westover MB, Hall LT, Deck GM, Cole AJ, Rosenthal ES. Metabolic correlates of the ictal-interictal continuum: FDG-PET during continuous EEG. Neurocrit Care 2016; 24: 324–31.

Taraseviciute A, Tkachev V, Ponce R, Turtle CJ, Snyder JM, Liggitt HD, et al. Chimeric antigen receptor T cell-mediated neurotoxicity in nonhuman primates. Cancer Discov 2018; 8: 750–63.

Torre M, Solomon IH, Sutherland CL, Nikiforow S, DeAngelo DJ, Stone RM, et al. Neuropathology of a case with fatal CAR T-cell-associated cerebral edema. J Neuropathol Exp Neurol 2018; 77: 877–82.

Turtle CJ, Hanafi LA, Berger C, Gooley TA, Cherian S, Hudecek M, et al. CD19 CAR-T cells of defined CD4+:CD8+ composition in adult B cell ALL patients. J Clin Invest 2016a; 126: 2123–38.

Turtle CJ, Hanafi LA, Berger C, Hudecek M, Pender B, Robinson E, et al. Immunotherapy of non-Hodgkin's lymphoma with a defined ratio of CD8+ and CD4+ CD19-specific chimeric antigen receptor-modified T cells. Sci Transl Med 2016b; 8: 355ra116.

Turtle CJ, Hay KA, Hanafi LA, Li D, Cherian S, Chen X, et al. Durable molecular remissions in chronic lymphocytic leukemia treated With CD19-specific chimeric antigen receptor-modified T cells after failure of ibrutinib. J Clin Oncol 2017; 35: 3010–20.

Vespa PM, McArthur DL, Xu Y, Eliseo M, Etchepare M, Dinov I, et al. Nonconvulsive seizures after traumatic brain injury are associated with hippocampal atrophy. Neurology 2010; 75: 792–8.

von Elm E, Altman DG, Egger M, Pocock SJ, Gøtzsche PC, Vandenbroucke JP. The Strengthening the Reporting of Observational Studies in Epidemiology (STROBE) statement: guidelines for reporting observational studies. Lancet 2007; 370: 1453–7.

Young GB, Jordan KG, Doig GS. An assessment of nonconvulsive seizures in the intensive care unit using continuous EEG monitoring: an investigation of variables associated with mortality. Neurology 1996; 47: 83–9.